

MISTUNING-BASED CONTROL DESIGN TO IMPROVE CLOSED-LOOP STABILITY OF VEHICULAR PLATOONS

Prabir Barooah, *Member, IEEE*, Prashant G. Mehta, *Member, IEEE* João P. Hespanha, *Member, IEEE*

Abstract

We consider a decentralized bidirectional control of a platoon of N identical vehicles moving in a straight line. The control objective is for each vehicle to maintain a constant velocity and inter-vehicular separation using only the local information from itself and its two nearest neighbors. Each vehicle is modeled as a double integrator. To aid the analysis, we use continuous approximation to derive a partial differential equation (PDE) approximation of the discrete platoon dynamics. The PDE model is used to explain the progressive loss of closed-loop stability with increasing number of vehicles, and to devise ways to combat this loss of stability.

If every vehicle uses the same controller, we show that the least stable closed-loop eigenvalue approaches zero as $O(\frac{1}{N^2})$ in the limit of a large number (N) of vehicles. We then show how to ameliorate this loss of stability margin by small amounts of “mistuning”, i.e., changing the controller gains from their nominal values. We prove that with arbitrary small amounts of mistuning, the asymptotic behavior of the least stable closed loop eigenvalue can be improved to $O(\frac{1}{N})$. All the conclusions drawn from analysis of the PDE model are corroborated via numerical calculations of the state-space platoon model.

I. INTRODUCTION

We consider the problem of controlling a one-dimensional platoon of N identical vehicles where the individual vehicles move at a constant pre-specified velocity V_d with an inter-vehicular spacing of Δ . Figure 1(a) illustrates the situation schematically. This problem is relevant to automated highway systems (AHS) because a controlled vehicular platoon with a constant but small inter-vehicular distance can help

Prabir Barooah is with the Dept. of Mechanical and Aerospace Engineering, University of Florida, Gainesville, FL 32611 (email: pbarooah@ufl.edu), Prashant G. Mehta is with the Dept. of Mechanical Science and Engineering, University of Illinois, Urbana-Champaign, IL 61801(email:mehtapg@uiuc.edu), and João P. Hespanha is with the Center for Control, Dynamical Systems, and Computation, University of California, Santa Barbara, CA 93106. (email: hespanha@ece.ucsb.edu)

Prabir Barooah and João Hespanha’s work was supported by the Institute for Collaborative Biotechnologies through grant DAAD19-03-D-0004 from the U.S. Army Research Office. Prashant Mehta’s work was supported by the National Science Foundation by grant CMS 05-56352.

improve the capacity (measured in vehicles/lane/hour, as in [1]) of a highway [2]. Due to this, the platoon control problem has been extensively studied [1, 3–7]. The dynamic and control issues in the platoon problem are also relevant to a general class of formation control problems including aerial vehicles, satellites *etc.* [8, 9].

Several approaches to the platoon control problem have been considered in the literature. These approaches fall into two broad categories depending on the information architecture available to the control algorithm(s): centralized and decentralized. In a decentralized architecture, the control action at any individual vehicle is computed based upon measurements obtained by on-board sensors, and possibly using wireless communication with a limited number of its neighbors. Decentralized architectures investigated in the literature include the predecessor-following [1, 10] and the bidirectional schemes [7, 11–14]. In the predecessor-following architecture, the control action at an individual vehicle depends only on the spacing error with the predecessor, i.e., the vehicle immediately ahead of it. In the bidirectional architecture, the control action depends upon relative position measurements from both the predecessor and the follower.

In a centralized architecture, measurements from all the vehicles are continually transmitted to a central controller or to all the vehicles. The optimal QR designs of [4, 6] typically lead to centralized architectures. Predecessor and Leader follower control schemes (see [15, 16] and references therein), which require global information from the first vehicle in the platoon are also examples of the centralized architecture. The high communication overhead in a centralized architecture makes it less attractive for platoons with a large number of vehicles. Additionally, with any centralized scheme, the closed loop system becomes sensitive to communication delays that are unavoidable with wireless communication [17].

The focus of this paper is on a decentralized bidirectional control architecture: the control action at an individual vehicle depends upon its own velocity and the relative position errors between itself and its predecessor and its follower vehicles. The decentralized bidirectional control architecture is advantageous because it is simple, modular, and it does not require continual inter-vehicular communication. Measurements needed for the control can be obtained by on-board sensors alone. Each vehicle is modeled as a double integrator. A double integrator model is common in the platoon control literature since the velocity dependent drag and other non-linear terms can usually be eliminated by feedback linearization [1, 10]. The control objective is to maintain a constant inter-vehicular spacing.

In spite of the advantages over centralized control, there are a number of challenges in the decentralized control of a platoon, especially when the number of vehicles, N , is large. First, the least stable closed-loop eigenvalue approaches zero as the number of vehicles increases [18]. Among decentralized schemes, one particularly important special case is the so-called *symmetric* bidirectional control, where all vehicles use identical controllers that are furthermore symmetric with respect to the predecessor and the follower position errors. In this case, the least stable closed loop eigenvalue approaches 0 as $O(\frac{1}{N^2})$ with a symmetric

bidirectional control and this behavior is independent of the choice of controller gains [18]. This progressive loss of closed-loop stability margin causes the closed loop performance of the platoon to become arbitrarily sluggish as the number of vehicles increases. It is interesting to note that the $O(\frac{1}{N^2})$ decay of the least stable eigenvalue occurs with the centralized LQR control as well [6].

The second challenge with decentralized control is that the sensitivity of the closed loop to external disturbances increases with increasing N . With predecessor following control, disturbance acting at an individual vehicle causes large spacing errors between other vehicle [1, 3, 19]. The seminal work of Darbha and Hedrick [19] on *string instability* was partly inspired by this issue. It was shown in [7] that sensitivity to disturbances with predecessor following control is independent of the choice of the controller. Similar controller-independent sensitivity to disturbances is also exhibited by the symmetric bidirectional architecture [7, 12]. In Yadlapalli *et al.* [20], it was shown that symmetric architectures have similarly poor sensitivity even when every vehicle uses information from more than two neighbors, as long as the number of neighbors is no more than $O(N^{2/3})$.

Third, there is a lack of design methods for decentralized architectures. For N vehicles, in general, N distinct controllers need to be designed, for which few control design methods exist. This has led to the examination of only the symmetric control among bidirectional architectures [7, 12, 20]. Some symmetry aided simplifications are possible for analysis and design in this case.

In summary, while issues such as stability and sensitivity to disturbances become critical as the platoon size increases, a lack of analysis and control design tools in decentralized settings makes it difficult to address these issues.

In this paper we present a novel analysis and design method for a decentralized bidirectional control architecture that ameliorates the progressive loss of closed loop stability margin with increasing number of vehicles. There are three contributions of this work that are summarized below.

First, we derive a partial differential equation (PDE) based continuous approximation of the (spatially) discrete platoon dynamics. Just as PDE can be discretized using a finite difference approximation, we carry out a reverse procedure: spatial difference terms in the discrete model are approximated by spatial derivatives. The resulting PDE yields the original set of ordinary differential equations upon discretization.

Two, we use the PDE model to derive a controller independent conclusion on stability with symmetric bi-directional architecture. In particular, the behavior of the least stable eigenvalue of the discrete platoon dynamics is predicted by analyzing the eigenvalues of the PDE. We show that the least stable closed-loop eigenvalue approaches zero as $O(\frac{1}{N^2})$. This prediction is confirmed by numerical evaluation of eigenvalues

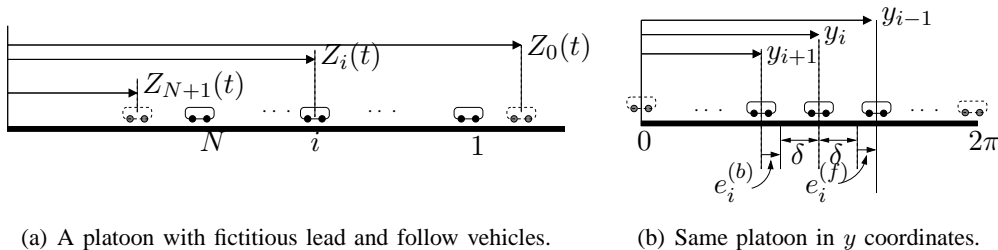
for both the PDE and the discrete platoon model. The real part of the least stable eigenvalue of the closed loop is taken as a measure of stability margin.

The third and the main contribution of the paper is a *mistuning-based control design* that leads to significant improvement in the closed loop stability margin over the symmetric case. The biggest advantage of using a PDE-based analysis is that the PDE reveals, better than the state-space model does, the mechanism of loss of stability margin and suggests a mistuning-based approach to ameliorate it. In particular, analysis of the PDE shows that forward-backward asymmetry in the control gains is beneficial. The asymmetry refers to the assignment of controller gains such that a vehicle utilizes information from the preceding and following vehicles differently. Our main results, Corollary 2 and Corollary 3, give control gains that achieve the best improvement in closed-loop stability by exploiting this asymmetry. In particular, we show that an arbitrarily small perturbation (asymmetry) in the controller gains from their values in the symmetric bidirectional case can result in the least stable eigenvalue approaching 0 only as $O(\frac{1}{N})$ (as opposed to $O(\frac{1}{N^2})$ in the symmetric bidirectional case). Numerical computations of eigenvalues of the state-space model of the platoon is used to confirm these predictions. Mistuning based approaches have been used for stability augmentation in many applications; see [21–24] for some recent references. Our paper is the first to consider such approaches in the context of decentralized control design.

Although the PDE model is derived under the assumption of large N , in practice the predictions of the PDE model match those of the state-space model accurately even for small values of N . Similarly, the benefits of mistuning are significant even for small values of N (see Section VI).

In addition to the stability margin improvements, the mistuning design reduces the closed loop’s sensitivity to external disturbances as well. In bidirectional architectures, the H_∞ norm of the transfer function from the external disturbances to the spacing errors is used as a measure of sensitivity to disturbances; cf., [7]. Numerical computation of the H_∞ norm of this transfer function shows that mistuning design also reduces sensitivity to disturbances significantly (see Section VI-D).

We briefly note that there is an extensive literature on modeling traffic dynamics using PDEs; see the seminal paper of Lighthill and Whitham [25] for an early reference, the paper of Helbing [26] and references therein for a survey of major approaches, and the papers of Jacquet *et al.* [27] and Li *et al.* [28] for control-oriented modeling. In spite of apparent similarities, our approach is quite different from the existing approaches. PDE models of traffic dynamics typically start with continuity and momentum equations [26]. Moreover, one requires a model of human behavior to determine an appropriate form of the external force in the momentum equation. This difficulty frequently leads to the introduction of terms in the PDE that are determined by fitting data; see [26, Section III-D] for a thorough discussion of such approximations used in various continuum traffic models. In contrast, we approximate the closed loop dynamic equations



(a) A platoon with fictitious lead and follow vehicles.

(b) Same platoon in y coordinates.Fig. 1. A platoon with N vehicles moving in one dimension.

by a continuous functions of space (and time) that is inspired by finite-difference discretization of PDEs. Ad-hoc approximations of human behavior is not needed. Moreover, the original dynamics can be recovered by discretizing the derived PDE, which provides further evidence of consistency between the (spatially) discrete and continuous models.

We also note that macroscopic models of traffic flow models have been used for designing control laws for a complete automated highway system (AHS) with lane changing, merging, etc. (see [28, 29] and references therein). The PDE model derived in the paper is not applicable to a complete AHS, but only to a single platoon.

The rest of the paper is organized as follows: Section II states the platoon problem in formal terms by describing a state-space model of the closed loop platoon dynamics; Section III then describes the derivation of the PDE model from the state space model. In Section IV the PDE is analyzed to explain the loss of stability margin with N when symmetric bidirection control is used. Section V describes how to ameliorate such loss of stability margin by mistuning. Section V-C reports simulation results that show the benefit of mistuning in time-domain. In Section VI, we comment on various aspects of the proposed mistuning-based design.

II. CLOSED LOOP DYNAMICS WITH BIDIRECTIONAL CONTROL

Consider a platoon of N identical vehicles moving in a straight line as shown schematically in Figure 1(a). Let $Z_i(t)$ and $V_i(t) := \dot{Z}_i(t)$ denote the position and the velocity, respectively, of the i^{th} vehicle for $i = 1, 2, \dots, N$. Each vehicle is modeled as a double integrator:

$$\ddot{Z}_i = U_i, \quad (1)$$

where U_i is the control (engine torque) applied on the i^{th} vehicle. Formally, such a model arises after the velocity dependent drag and other non-linear terms have been eliminated by using feedback linearization [1, 10].

Scenario	Length L	Leader	Follower
I	$(N + 1)\Delta$	$\tilde{v}_0 = 0$	$\tilde{v}_{N+1} = 0$
II	$N\Delta$	$\tilde{v}_0 = 0$	–

TABLE I
THE TWO SCENARIOS.

The control objective is to maintain a constant inter-vehicular distance Δ and a constant velocity V_d for every vehicle. Every vehicle is assumed to know the desired spacing Δ and the desired velocity V_d . The control architecture is required to be decentralized, so that every vehicle uses locally available measurements. We assume that the error between the position (as well as velocity) of a vehicle and its desired value is small, so that analysis of the platoon dynamics with linear vehicle model and linear control law is justified.

In this paper, we assume a bi-directional control architecture for individual vehicles in the platoon (except the first and the last vehicles). For the first and the last vehicles, we consider two types of control architectures (termed as scenarios I and II) as tabulated in Table I. In scenario I, we introduce (after [5, 6]) a fictitious lead vehicle and a fictitious follow vehicle, indexed as 0 and $N + 1$ respectively. Their behavior is specified by imposing a constant velocity trajectories as $Z_0(t) = V_d t$ and $Z_{N+1} = V_d t - (N + 1)\Delta$. In scenario II, only a fictitious lead vehicle with index $i = 0$ with $Z_0(t) = V_d t$ is introduced. For the last vehicle in the platoon in scenario II, there is no follower vehicle and it uses information only from its predecessor to maintain a constant gap.

Consistent with the decentralized bidirectional linear control architecture, the control U_i for the i^{th} vehicle is assumed to depend only on 1) its velocity error $V_i - V_d$, and 2) the relative position errors between itself and its immediate neighbors. That is,

$$U_i = k_i^{(f)}(Z_{i-1} - Z_i - \Delta) - k_i^{(b)}(Z_i - Z_{i+1} - \Delta) - b_i(V_i - V_d). \quad (2)$$

where $k_i^{(\cdot)}$, b_i are positive constants. The first two terms are used to compensate for any deviation away from nominal with the predecessor (front) and the follower (back) vehicles respectively. The superscripts (f) and (b) correspond to *front* and *back*, respectively. The third term is used to obtain a zero steady-state error in velocity. In principle, relative velocity errors between neighboring vehicles can also be incorporated into the control, but we do not examine this situation here. Since V_d and Δ are known to every vehicle, the relative

errors used in the control law, including the velocity error, can be obtained in practice by on-board devices such as radars, GPS, and speed sensors.

The control law (2) represents state feedback with only local (nearest neighbor) information. Analysis of this controller structure is relevant even if there are additional dynamic elements in the controller. There are several reasons for this. First, a dynamic controller cannot have a zero at the origin. It will result in a pole-zero cancelation causing the steady-state errors to grow without bound as N increases [12]. Second, a dynamic controller cannot have an integrator either. For if it does, the closed-loop platoon dynamics become unstable for a sufficiently large values of N [12]. As a result, any allowable dynamic compensator must essentially act as a static gain at low frequencies. The results of [12] indicate that the principal challenge in controlling large platoons arises due to the presence of a double integrator with its unbounded gain at low frequencies. Hence, the limitation and its amelioration discussed here with the local state feedback structure of (6) is also relevant to the case where additional dynamic elements appear in the control.

To facilitate analysis, we consider a coordinate change

$$y_i = 2\pi\left(\frac{Z_i(t) - V_d t + L}{L}\right), \quad v_i = 2\pi\frac{V_i - V_d}{L}, \quad (3)$$

where L denotes the platoon length, which equals $(N+1)\Delta$ in scenario I and $N\Delta$ in scenario II. Figure 1(b) depicts the schematic of the platoon in the new coordinates. The scaling ensures that $y_0(t) \equiv 2\pi$, $y_i(t) \in [0, 2\pi]$, and $y_{N+1}(t) \equiv 0$ ($y_N(t) = 0$) in scenario I (II). Here, we have implicitly assumed that deviations of the vehicle positions and velocities from their desired values are small.

In the scaled coordinate, the dynamics of the i^{th} vehicle are described by

$$\ddot{y}_i = u_i, \quad (4)$$

where $u_i := 2\pi U_i/L$. The desired spacing and velocities are

$$\delta := \frac{\Delta}{L/2\pi}, \quad v_d := \frac{V_d - V_d}{L/2\pi} = 0,$$

and the desired position of the i^{th} vehicle is

$$y_i^d(t) \equiv 2\pi - i\delta. \quad (5)$$

The position and velocity errors for the i^{th} vehicle are given by:

$$\tilde{y}_i(t) = y_i(t) - y_i^d(t), \quad \tilde{v}_i = v_i - v_d = v_i, \quad \text{and } \dot{\tilde{y}}_i = \dot{y}_i.$$

We note that $\tilde{v}_0 = \tilde{v}_{N+1} = 0$ for the fictitious lead and follow vehicles. In the scaled coordinates, the decentralized bidirectional control law (2) is equivalent to the following

$$u_i = k_i^{(f)}(y_{i-1} - y_i - \delta) - k_i^{(b)}(y_i - y_{i+1} - \delta) - b_i \tilde{v}_i \quad (6)$$

$$= k_i^{(f)}(\tilde{y}_{i-1} - \tilde{y}_i) - k_i^{(b)}(\tilde{y}_i - \tilde{y}_{i+1}) - b_i \tilde{v}_i. \quad (7)$$

It follows from (4) and (6) that the closed loop dynamics of the i^{th} vehicle in the \tilde{y} -coordinate is

$$\ddot{\tilde{y}}_i + b_i \dot{\tilde{y}}_i = k_i^{(f)} (\tilde{y}_{i-1} - \tilde{y}_i) - k_i^{(b)} (\tilde{y}_i - \tilde{y}_{i+1}). \quad (8)$$

To describe the closed-loop dynamics of the whole platoon, we define

$$\tilde{\mathbf{y}} := [\tilde{y}_1, \tilde{y}_2, \dots, \tilde{y}_N]^T, \quad \tilde{\mathbf{v}} := [\tilde{v}_1, \dots, \tilde{v}_N]^T.$$

For scenario I with fictitious lead and follow vehicles, the control law (6) yields the following closed loop dynamics.

$$\begin{bmatrix} \dot{\tilde{\mathbf{y}}} \\ \dot{\tilde{\mathbf{v}}} \end{bmatrix} = \underbrace{\begin{bmatrix} 0 & I \\ -K_I^{(f)} M^T - K_I^{(b)} M & -B \end{bmatrix}}_{A_{L-F}} \begin{bmatrix} \tilde{\mathbf{y}} \\ \tilde{\mathbf{v}} \end{bmatrix} \quad (9)$$

where $K_I^{(f)} = \text{diag}(k_1^{(f)}, k_2^{(f)}, \dots, k_N^{(f)})$, $K_I^{(b)} = \text{diag}(k_1^{(b)}, k_2^{(b)}, \dots, k_N^{(b)})$, $B = \text{diag}(b_1, b_2, \dots, b_N)$, and

$$M = \begin{bmatrix} 1 & -1 & 0 & \dots \\ 0 & 1 & -1 & \dots \\ \vdots & & \ddots & \ddots \\ \dots & & & 1 & -1 \\ \dots & & & 0 & 1 \end{bmatrix}.$$

For scenario II with a fictitious lead vehicle and no follow vehicle, the closed loop dynamics are

$$\begin{bmatrix} \dot{\tilde{\mathbf{y}}} \\ \dot{\tilde{\mathbf{v}}} \end{bmatrix} = \underbrace{\begin{bmatrix} 0 & I \\ -K_{II}^{(f)} M^T - K_{II}^{(b)} M_o & -B \end{bmatrix}}_{A_L} \begin{bmatrix} \tilde{\mathbf{y}} \\ \tilde{\mathbf{v}} \end{bmatrix}, \quad (10)$$

where $K_{II}^{(f)} = K_I^{(f)}$, $K_{II}^{(b)} = \text{diag}(k_1^{(b)}, k_2^{(b)}, \dots, k_{N-1}^{(b)}, 0)$, and

$$M_o = \begin{bmatrix} 1 & -1 & 0 & \dots \\ 0 & 1 & -1 & \dots \\ \vdots & & \ddots & \ddots \\ \dots & & & 1 & -1 \\ \dots & & & 0 & 0 \end{bmatrix}.$$

Our goal is to understand the behavior of the closed loop stability margin with increasing N and to devise ways to improve it by appropriately choosing the controller gains. While in principle this can be done by analyzing the eigenvalues of the matrix A_{L-F} (scenario I) and of A_L (scenario II), we take an alternate route. For large values of N , we approximate the dynamics of the discrete platoon by a partial differential equation (PDE) which is used for analysis and control design.

III. PDE MODEL OF PLATOON CLOSED LOOP DYNAMICS

In this section, we develop a continuous PDE approximation of the (spatially) discrete platoon dynamics. The PDE is derived with respect to a scaled spatial coordinate $x \in [0, 2\pi]$. We recall that in Section II, the scaled location of the i^{th} vehicle (denoted as y_i) too was defined with respect to such a coordinate system. In effect, the two symbols x and y correspond to the same coordinate representation but are used here to distinguish the continuous and discrete formulations. As in the discrete case, the platoon always occupies a length of 2π irrespective of N .

A. PDE derivation

The starting point is a continuous approximation:

$$v(x, t) := v_i(t), \quad \text{at } x = y_i. \quad (11)$$

Similarly, $b(x)$, $k^{(f)}(x)$, $k^{(b)}(x)$ are used to denote continuous approximations of discrete gains b_i , $k_i^{(f)}$, $k_i^{(b)}$ respectively. We will construct a PDE approximation of discrete dynamics in terms of these continuous approximations. To do so, it is convenient to first differentiate (8) with respect to time,

$$\ddot{v}_i + b_i \dot{v}_i = k_i^{(f)}(\tilde{v}_{i-1} - \tilde{v}_i) - k_i^{(b)}(\tilde{v}_i - \tilde{v}_{i+1}). \quad (12)$$

We recast this equation

$$\ddot{v}_i + b_i \dot{v}_i = -k_i^{(+)}v_i + \frac{1}{2}(k_i^{(+)} + k_i^{(-)})v_{i-1} - \frac{1}{2}(k_i^{(+)} - k_i^{(-)})v_{i+1},$$

where

$$k_i^{(+)} := k_i^{(f)} + k_i^{(b)}, \quad k_i^{(-)} := k_i^{(f)} - k_i^{(b)}. \quad (13)$$

It follows that

$$\begin{aligned} \ddot{v}_i + b_i \dot{v}_i &= \frac{1}{2}k_i^{(-)}(v_{i-1} - v_{i+1}) + \frac{1}{2}k_i^{(+)}(v_{i-1} - 2v_i + v_{i+1}) \\ &= \frac{1}{\rho_0}k_i^{(-)}\frac{v_{i-1} - v_{i+1}}{2\delta} + \frac{1}{2\rho_0^2}k_i^{(+)}\frac{v_{i-1} - 2v_i + v_{i+1}}{\delta_0^2} \end{aligned}$$

where

$$\rho_0 := \frac{1}{\delta} = \frac{N}{2\pi}. \quad (14)$$

ρ_0 has the physical interpretation of the *mean density* (vehicles per unit length). Now, we make a finite-difference approximation of derivatives

$$\begin{aligned} \frac{v_{i-1} - v_{i+1}}{2\delta} &= \left[\frac{\partial}{\partial x} v(x, t) \right]_{x=y_i} \\ \frac{v_{i-1} - 2v_i + v_{i+1}}{\delta_0^2} &= \left[\frac{\partial^2}{\partial x^2} v(x, t) \right]_{x=y_i}, \end{aligned}$$

where we recall that $v(x, t)$ is a continuous approximation of the vehicle velocities ($v_i(t) = v(y_i, t)$ etc). Denoting $k^{(+)}(x)$ and $k^{(-)}(x)$ as continuous approximations of $k_i^{(+)}$ and $k_i^{(-)}$ respectively, the discrete model is written as:

$$\left[\frac{\partial^2}{\partial t^2} v(x, t) \right]_{x=y_i} + \left[b(x) \frac{\partial}{\partial t} v(x, t) \right]_{x=y_i} = \frac{1}{\rho_0} \left[k^{(-)}(x) \frac{\partial}{\partial x} v(x, t) \right]_{x=y_i} + \frac{1}{2\rho_0^2} \left[k^{(+)}(x) \frac{\partial^2}{\partial x^2} v(x, t) \right]_{x=y_i}$$

Hence, we arrive at the partial differential equation (PDE) as a model of the discrete platoon dynamics:

$$\left(\frac{\partial^2}{\partial t^2} + b(x) \frac{\partial}{\partial t} \right) v(x, t) = \left(\frac{1}{\rho_0} k^{(-)}(x) \frac{\partial}{\partial x} + \frac{1}{2\rho_0^2} k^{(+)}(x) \frac{\partial^2}{\partial x^2} \right) v(x, t) \quad (15)$$

In the remainder of this paper, we assume that $k^{(+)}(x) > 0$. Using (13), the continuous counterparts of the front and the back gains are given by

$$\begin{aligned} k^{(f)}(x) &= \frac{1}{2} \left(k^{(+)}(x) + k^{(-)}(x) \right), \\ k^{(b)}(x) &= \frac{1}{2} \left(k^{(+)}(x) - k^{(-)}(x) \right), \end{aligned} \quad (16)$$

so that the gain values $k_i^{(\cdot)}$ can be obtained as $k_i^{(f)} = k^{(f)}(y_i)$ and $k_i^{(b)} = k^{(b)}(y_i)$. It can be readily verified that one recovers the system of ordinary differential equation ((12) for $i = 1, \dots, N$) by discretizing the PDE (15) using a finite difference scheme on the interval $[0, 2\pi]$ with a discretization δ between discrete points.

The boundary conditions for the PDE (15) depend upon the dynamics of the first and the last vehicles in the platoon. For scenario I with a constant velocity fictitious lead and follow vehicles, the appropriate boundary conditions are of the Dirichlet type on both ends:

$$\tilde{v}(0, t) = \tilde{v}(2\pi, t) = 0, \quad \forall t \in [0, \infty). \quad (17)$$

For scenario II with the only a fictitious lead vehicle, the appropriate boundary conditions are of Neumann-Dirichlet type:

$$\frac{\partial \tilde{v}}{\partial x}(0, t) = \tilde{v}(2\pi, t) = 0. \quad \forall t \in [0, \infty) \quad (18)$$

We refer the reader to Appendix I-A for a discussion on well-posedness of the solutions to (15). It is shown in Appendix I-A that a solution exists in a weak sense when $k^{(+)}, k^{(-)}, \frac{dk^{(+)}}{dx} \in L^\infty([0, 2\pi])$.

B. Eigenvalue comparison

For preliminary comparison of the PDE obtained above with the state-space model of the closed loop platoon dynamics, we consider the simplest case where the position control gains are constant for every vehicle, i.e., $k^{(f)}(x) = k^{(b)}(x) = k_0$ and $b(x) = b_0$. In such a case $k^{(-)}(x) \equiv 0$, $k^{(+)}(x) \equiv 2k_0$ and the PDE (15) simplifies to

$$\left(\frac{\partial^2}{\partial t^2} + b_0 \frac{\partial}{\partial t} - \frac{k_0}{\rho_0^2} \frac{\partial^2}{\partial x^2} \right) \tilde{v} = 0, \quad (19)$$

which is a damped wave equation with a wave speed of $\frac{\sqrt{k_0}}{\rho_0}$. The wave equation is consistent with the physical intuition that a symmetric bidirectional control architecture causes a disturbance to propagate equally in both directions.

Figure 2 compares the closed loop eigenvalues of a discrete platoon with $N = 25$ vehicles and the PDE (19). The eigenvalues of the platoon are obtained by numerically evaluating the eigenvalues of the matrices A_{L-F} and A_L (defined in (9) and (10)). The eigenvalues of the PDE are computed numerically

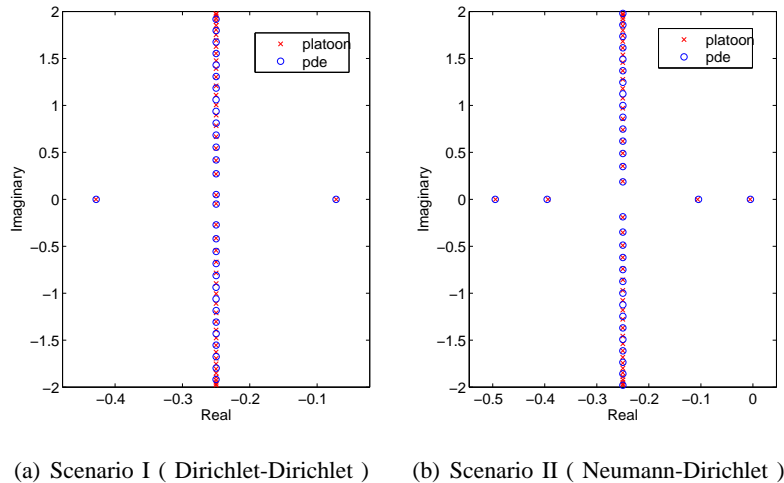


Fig. 2. Comparison of closed loop eigenvalues of the platoon dynamics and the eigenvalues of the corresponding PDE (19) for the two different scenarios: (a) platoon with fictitious lead and follow vehicles, and correspondingly the PDE (19) with Dirichlet boundary conditions, (b) platoon with fictitious lead vehicle, and correspondingly the PDE (19) with Neumann-Dirichlet boundary conditions. For ease of comparison, only a few of the eigenvalues are shown. Both plots are for $N = 25$ vehicles; the controller parameters are $k_i^{(f)} = k_i^{(b)} = 1$ and $b_i = 0.5$ for $i = 1, 2, \dots, N$, and for the PDE $k^{(f)}(x) \equiv k^{(b)}(x) \equiv 1$ and $b(x) \equiv 0.5$.

after using a Galerkin method with Fourier basis [30]. The figure shows that the two sets of eigenvalues are in excellent match. In particular, the least stable eigenvalues are well-captured by the PDE. Additional comparison appears in the following sections, where we present the results for analysis and control design.

IV. ANALYSIS OF THE SYMMETRIC BIDIRECTIONAL CASE

This section is concerned with asymptotic formulas for stability margin (least stable eigenvalue) for the symmetric bidirectional architecture with symmetric and constant control gains: $k^{(f)}(x) = k^{(b)}(x) \equiv k_0$ and $b(x) \equiv b_0$. The analysis is carried out with the aid of the associated PDE model:

$$\left(\frac{\partial^2}{\partial t^2} + b_0 \frac{\partial}{\partial t} - a_0^2 \frac{\partial^2}{\partial x^2} \right) \tilde{v} = 0, \quad (20)$$

where $x \in [0, 2\pi]$ and

$$a_0^2 := \frac{k_0}{\rho_0^2} \quad (21)$$

is the wave speed. The closed-loop eigenvalues of the PDE model require consideration of the eigenvalue problem

$$\frac{d^2 \eta}{dx^2} = \lambda \eta(x), \quad (22)$$

boundary condition	eigenvalue λ_l	eigenfunction $\psi_l(x)$	l
$\eta(0) = \eta(2\pi) = 0$ (Dirichlet - Dirichlet)	$-\frac{l^2}{4}$	$\sin(\frac{lx}{2})$	$l = 1, 2, \dots$
$\frac{\partial \eta}{\partial x}(0) = \eta(2\pi) = 0$ (Neumann - Dirichlet)	$-\frac{(2l-1)^2}{16}$	$\cos(\frac{(2l-1)x}{4})$	$l = 1, 2, \dots$

TABLE II

THE EIGEN-SOLUTIONS FOR THE LAPLACIAN OPERATOR WITH TWO DIFFERENT BOUNDARY CONDITIONS.

and η is an eigenfunction that satisfies appropriate boundary conditions: (17) for scenario I and (18) for scenario II. The eigensolutions to the eigenvalue problem (22) for the two scenarios are given in Table II. The eigenfunctions in either scenario provide a basis of $L^2([0, 2\pi])$.

After taking a Laplace transform, the eigenvalues of the PDE model (20) are obtained as roots of the characteristic equation

$$s^2 + b_0 s - a_0^2 \lambda = 0, \quad (23)$$

where λ satisfies (22). Using Table II, these roots are easily evaluated. For instance, the l^{th} eigenvalue of the PDE with Dirichlet boundary conditions is given by

$$s_l^\pm = \frac{-b_0 \pm \sqrt{b_0^2 - a_0^2 l^2}}{2}, \quad (24)$$

where $l = 1, 2, \dots$. The real part of the eigenvalue depends upon the discriminant $D(l, N) = (b_0^2 - a_0^2 l^2)$, where the wave speed a_0 depends both on control gain k_0 and number of vehicles N (see (21)). For a fixed control gain, there are two cases to consider:

- 1) If $D(l, N) < 0$, the roots s_l^\pm are complex with the real part given by $-\frac{b_0}{2}$,
- 2) If $D(l, N) > 0$, the roots s_l^\pm are real with $s_l^+ + s_l^- = -b_0$.

In the former case, the damping is determined by the velocity feedback term $b_0 \frac{\partial}{\partial t}$, while in the latter case one eigenvalue (s_l^-) gains damping at the expense of the other (s_l^+) which loses damping. When s_l^\pm are real, the eigenvalue s_l^+ is closer to the origin than s_l^- ; so we call s_l^+ the l^{th} *less-stable* eigenvalue. The following lemma gives the asymptotic formula for this eigenvalue in the limit of large N .

boundary condition	s_l^+ for $l \ll l_c$	l_c
Dirichlet-Dirichlet	$-\frac{\pi^2 k_0}{b_0} \frac{l^2}{N^2} + O(\frac{1}{N^4})$	$\frac{b_0 N}{2\pi\sqrt{k_0}}$
Neumann-Dirichlet	$-\frac{\pi^2 k_0}{4b_0} \frac{l^2}{N^2} + O(\frac{1}{N^4})$	$\frac{b_0 N}{2\pi\sqrt{k_0}}$

TABLE III

THE TREND OF THE LESS STABLE EIGENVALUE s_l^+ FOR THE PDE (20)

Lemma 1: Consider the eigenvalue problem for the linear PDE (20) with boundary conditions (17) and (18), corresponding to scenarios I and II respectively. The l^{th} less-stable eigenvalue s_l^+ approaches 0 as $O(1/N^2)$ in the limit as $N \rightarrow \infty$. The asymptotic formulas appear in Table III. \square

Proof of Lemma 1. We first consider scenario I with Dirichlet boundary conditions (17). Using (24) and (21),

$$2s_l^\pm = -b_0 \pm b_0 \left(1 - \frac{a_0^2 l^2}{b_0^2}\right)^{1/2} = -b_0 \pm b_0 \left(1 - \frac{2\pi^2 k_0}{b_0^2} \frac{l^2}{N^2}\right) + O\left(\frac{1}{N^4}\right)$$

for $a_0^2 l^2 / b_0^2 \ll 1$. The asymptotic formula holds for wave numbers

$$l \ll \frac{b_0}{a_0} = \frac{b_0 N}{2\pi\sqrt{k_0}} =: l_c, \quad (25)$$

and in particular for each l as $N \rightarrow \infty$. The proof for the scenario II with Neumann-Dirichlet boundary conditions (18) follows similarly. \blacksquare

The stability margin of the platoon can be measured by the real part of s_1^+ , the *least stable eigenvalue*.

Corollary 1: Consider the eigenvalue problem for the linear PDE (20) with boundary conditions (17) and (18), corresponding to scenarios I and II respectively. The least stable eigenvalue, denoted by s_1^+ , satisfies

$$s_1^+ = -\frac{\pi^2 k_0}{b_0} \frac{1}{N^2} + O\left(\frac{1}{N^4}\right) \quad (\text{Dirichlet-Dirichlet}) \quad (26)$$

$$s_1^+ = -\frac{\pi^2 k_0}{4b_0} \frac{1}{N^2} + O\left(\frac{1}{N^4}\right) \quad (\text{Neumann-Dirichlet}) \quad (27)$$

as $N \rightarrow \infty$. \square

The result shows that the least stable eigenvalue of the closed loop platoon decays as $O(\frac{1}{N^2})$ with symmetric bidirectional control.

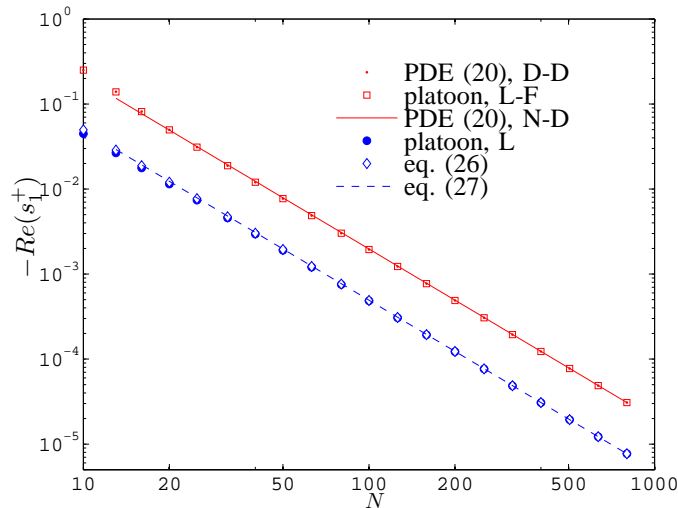


Fig. 3. Comparison of the least stable eigenvalue of the closed loop platoon dynamics and that predicted by Corollary 1 with symmetric bidirectional control. In the plot legends, “D-D” stands for “Dirichlet-Dirichlet”, “N-D” for “Neumann-Dirichlet”, “L-F” for fictitious leader-follower, and “L” for fictitious leader. The plot for “PDE (20), D-D” should be compared with “platoon, L-F” since they both correspond to scenario I. Similarly, “PDE (20), N-D” and “platoon, L” correspond to scenario II. Note that the predictions (26) and (27) are valid for $1 \ll l_c$ (defined in (25)), which in this case means for $N \gg 12$.

We now present numerical computations that corroborates this PDE-based analysis. Figure 3 plots as a function of N the least stable eigenvalue of the PDE and of the state-space model of the platoon, as well as the prediction from the asymptotic formula. The eigenvalues for the discrete platoon are obtained by numerically evaluating the eigenvalues of the matrices A_{L-F} and A_L (see (9) and (10)) with constant control gains $k_i^{(f)} = k_i^{(b)} = k_0 = 1$ and $b_i = b_0 = 0.5$ for $i = 1, \dots, N$. The comparison shows that the PDE analysis accurately predicts the eigenvalue of the state-space model of the platoon dynamics.

Figure 4(a) graphically illustrates the destabilization by depicting the movement of eigenvalues s_1^\pm as N increases. For sufficiently small values of N , the discriminant $D(1, N)$ is negative and the eigenvalue s_1^\pm are complex. The real part of the eigenvalue depends only on the value of b_0 . At a critical value of $N = N_c := \frac{\pi\sqrt{2k_0}}{b_0}$, the discriminant becomes zero, $s_1^+ = s_1^-$ and the eigenvalues collide on the real axis. For values of $N > N_c$ and in particular as $N \rightarrow \infty$, the eigenvalue s_1^+ asymptotes to 0 while staying real, and s_1^- asymptotes to $-b$. Their cumulative damping, as reflected in the sum $s_1^+ + s_1^- = -b_0$, is conserved. In other words, s_1^+ is destabilized at the expense of s_1^- .

Remark 1: The preceding analysis shows that the loss of stability experienced with a symmetric bidirec-

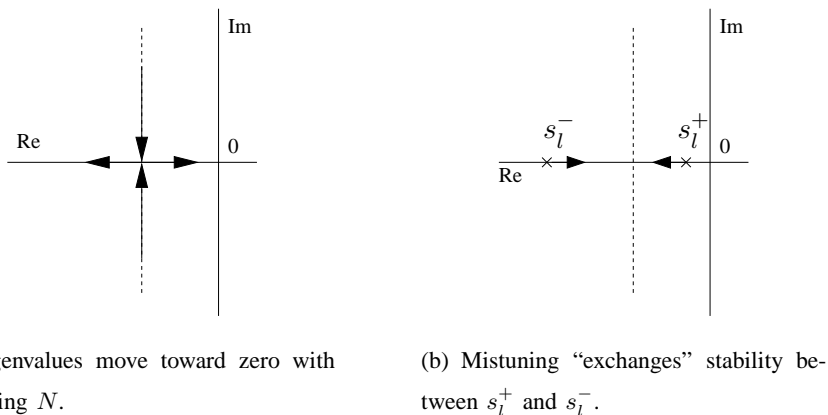


Fig. 4. A schematic explaining the loss of stability as N increases and how mistuning ameliorates this loss.

tional architecture is controller independent. The least stable eigenvalue approaches 0 as $O(1/N^2)$ irrespective of the values of the gains k_0 and b_0 , as long as they are fixed constants independent of N . Corollary 1 also implies that for the least stable eigenvalue to be uniformly bounded away from 0, one has to increase the control gain k_0 as N^2 . In Jovanović and Bamieh [6], the same conclusion was reached for the least stable eigenvalue with LQR control of a platoon on a circle. LQR control typically leads to a centralized architecture, whereas symmetric bidirectional control is decentralized. It is interesting to note that the least stable eigenvalue behaves similarly in these distinct architectures. \square

V. REDUCING LOSS OF STABILITY BY MISTUNING

In this section, we examine the problem of designing the control gain functions $k^{(f)}(x), k^{(b)}(x)$ so as to ameliorate the loss of stability margin with increasing N that was seen in the previous sections when $k^{(f)}(x) = k^{(b)} \equiv k_0$. Specifically, we consider the eigenvalue problem for the PDE (15) where the control gains are changed slightly (mistuned) from their values in the symmetric bidirectional case in order to minimize the least-stable eigenvalue s_1^+ . With symmetric bidirectional control, one obtains an $O(\frac{1}{N^2})$ estimate for the least stable eigenvalue because the coefficient of $\frac{\partial^2}{\partial x^2}$ term in PDE (15) is $O(\frac{1}{N^2})$ and the coefficient of $\frac{\partial}{\partial x}$ term is 0. Any asymmetry between the forward and the backward gains will lead to non-zero $k^{(-)}(x)$ and a presence of $O(\frac{1}{N})$ term as coefficient of $\frac{\partial}{\partial x}$. By a judicious choice of asymmetry, there is thus a potential to improve the stability margin from $O(\frac{1}{N^2})$ to $O(\frac{1}{N})$.

We begin by considering the forward and backward position feedback gain profiles:

$$k^{(f)}(x) = k_0 + \epsilon k^{(f,purt)}(x),$$

$$k^{(b)}(x) = k_0 + \epsilon k^{(b,purt)}(x),$$

where $\epsilon > 0$ is a small parameter signifying the amount of mistuning and $k^{(f,purt)}(x)$, $k^{(b,purt)}(x)$ are functions defined over the interval $[0, 2\pi]$ that capture *perturbation* from the nominal value k_0 . Define

$$\begin{aligned} k_s(x) &:= k^{(f,purt)}(x) + k^{(b,purt)}(x), \\ k_m(x) &:= k^{(f,purt)}(x) - k^{(b,purt)}(x), \end{aligned}$$

so that from (16),

$$\begin{aligned} k^{(+)}(x) &= 2k_0 + \epsilon k_s(x), \\ k^{(-)}(x) &= \epsilon k_m(x). \end{aligned}$$

The mistuned version of the PDE (15) is then given by

$$\frac{\partial^2 \tilde{v}}{\partial t^2} + b_0 \frac{\partial \tilde{v}}{\partial t} = a_0^2 \frac{\partial^2 \tilde{v}}{\partial x^2} + \epsilon \left[\frac{k_m}{\rho_0} \frac{\partial \tilde{v}}{\partial x} + \frac{k_s}{2\rho_0^2} \frac{\partial^2 \tilde{v}}{\partial x^2} \right] \quad (28)$$

We study the problem of improving the stability margin by judicious choice of $k_m(x)$ and $k_s(x)$. The results of our investigation, carried out in the following sections, provide a systematic framework for designing control gains in the platoon by introducing small changes to the symmetric design.

A. Mistuning-based design for scenario I

The control objective is to design mistuning profiles $k_m(x)$ and $k_s(x)$ to *minimize* the least stable eigenvalue s_1^+ . To achieve this, we first obtain an explicit asymptotic formula for the eigenvalues when a small amount of asymmetry is introduced in the control gains (i.e., when ϵ is small). For scenario I, the result is presented in the following theorem. The proof appears in Appendix I-B.

Theorem 1: Consider the eigenvalue problem for the mistuned PDE (28) with Dirichlet boundary condition (17) corresponding to scenario I. The l^{th} eigenvalue pair is given by the asymptotic formula

$$\begin{aligned} s_l^+(\epsilon) &= \epsilon \frac{l}{2b_0 N} \int_0^{2\pi} k_m(x) \sin(lx) dx + O(\epsilon^2) + O\left(\frac{1}{N^2}\right), \\ s_l^-(\epsilon) &= -b_0 - \epsilon \frac{l}{2b_0 N} \int_0^{2\pi} k_m(x) \sin(lx) dx + O(\epsilon^2) + O\left(\frac{1}{N^2}\right), \end{aligned}$$

that is valid for each l in the limit as $\epsilon \rightarrow 0$ and $N \rightarrow \infty$. \square

It is apparent from the theorem above that to minimize the least stable eigenvalue s_1^+ , one needs to choose only k_m carefully; k_s has only $O(\frac{1}{N^2})$ effect. Therefore we choose $k_s(x) \equiv 0$, or, equivalently, $k^{(f,purt)}(x) = -k^{(b,purt)}(x)$, which leads to $k_m(x) = 2k^{(f,purt)}(x)$. The most beneficial control gains are now can be readily obtained from Theorem 1, which is summarized in the next corollary.

Corollary 2 (Mistuning profile for Scenario I): Consider the problem of minimizing the least-stable eigenvalue of the PDE (28) with Dirichlet boundary condition (17) by choosing $k^{(f,purt)}(x) \in L^\infty([0, 2\pi])$ with

norm-constraint $\|k^{(f, \text{purt})}(x)\|_{L^\infty} = \max_{x \in [0, 2\pi]} |k^{(f, \text{purt})}(x)| = 1$ and $k^{(b, \text{purt})}(x) = -k^{(f, \text{purt})}(x)$. In the limit as $\epsilon \rightarrow 0$, the optimal mistuning profile is given by $k^{(f, \text{purt})}(x) = -2(H(x - \pi) - \frac{1}{2})$, where $H(x)$ is the Heaviside function: $H(x) = 1$ for $x \geq 0$ and $H(x) = 0$ for $x < 0$. With this profile, the least stable eigenvalue is given by the asymptotic formula

$$s_1^+(\epsilon) = -\frac{4\epsilon}{b_0 N}$$

in the limit as $\epsilon \rightarrow 0$ and $N \rightarrow \infty$. □

The result shows that even with an *arbitrarily small amount* of mistuning ϵ , one can improve the closed-loop platoon stability margin by a large amount, especially for large values of N . The least-stable eigenvalue s_1^+ asymptotes to 0 as $O(\frac{1}{N})$ in the mistuned case as opposed to $O(\frac{1}{N^2})$ in the symmetric case.

Figure 5(a) shows the control gains for the individual vehicles (that are obtained from sampling the functions $k^{(f)}(x)$ and $k^{(b)}(x)$), suggested by Corollary 2 for a 20 vehicle platoon, with $k_0 = 1$ and $\epsilon = 0.1$. A confirmation of the predictions of Corollary 2 is presented in Figure 6. Numerically obtained mistuned and nominal eigenvalues for both the PDE and the platoon state-space model are shown in the figure, with mistuned gains chosen as shown in Figure 5(a). The figure shows that

- 1) the platoon eigenvalues match the PDE eigenvalues accurately over a range of N , and
- 2) the mistuned eigenvalues show large improvement over the nominal case even though the controller gains differ from their nominal values only by $\pm 10\%$. The improvement is particularly noticeable for large values of N , while being significant even for small values of N .

For comparison, the figure also depicts the asymptotic eigenvalue formula given in Corollary 2.

Figure 4(b) graphically illustrates the mechanism by which mistuning affects the movement of eigenvalues s_1^\pm as N increases. By properly choosing the mistuning patterns $k_m(x)$ and $k_s(x)$, damping can be “exchanged” between the eigenvalues s_1^+ and s_1^- so that the less stable eigenvalue s_1^+ “gains” stability at the expense of the more stable eigenvalue s_1^- . The net amount of damping is preserved, since $s_1^+ + s_1^- = -b_0$ (as seen from Theorem 1).

B. Mistuning-based design for scenario II

For scenario II, asymptotic formula for the eigenvalue (counterpart of Theorem 1) is summarized in the following theorem. The proof is entirely analogous to the proof of Theorem 1, and is therefore omitted.

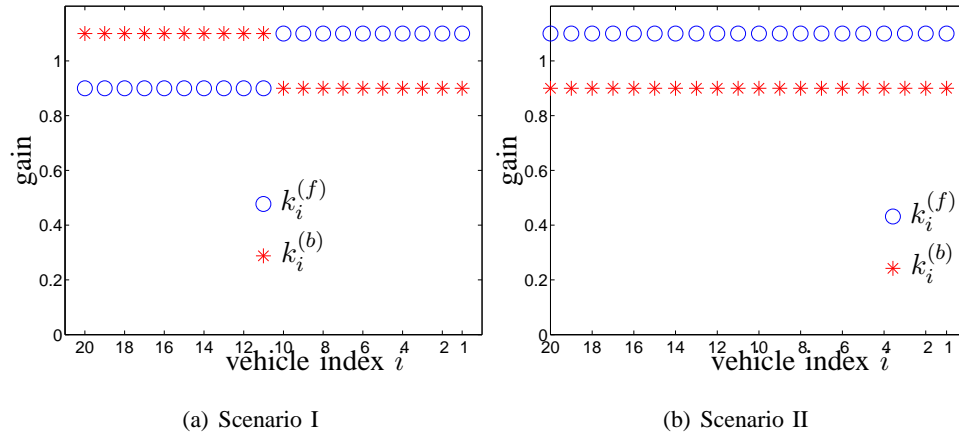


Fig. 5. Mistuned front and back gains $k_i^{(f)}$ and $k_i^{(b)}$ of the vehicles in a platoon with $k_0 = 1$ and $\epsilon = 0.1$. Figure (a) shows the gains chosen according to Corollary 2 to be optimal for scenario I for small ϵ : $k_i^{(f)} = k_0 (1 - 0.1(2H(y_i^d - \pi) - 1))$, $k_i^{(b)} = k_0 (1 + 0.1(2H(y_i^d - \pi) - 1))$, where $H(\cdot)$ is the Heaviside function and y_i^d defined in (5) is the desired position of the i^{th} vehicle. Figure (b) shows the optimal mistuned gains for scenario II with the same parameters, which turns out to be (see Corollary 3) $k_i^{(f)} = 1.1k_0$ and $k_i^{(b)} = 0.9k_0$ for $i = 1, \dots, N$.

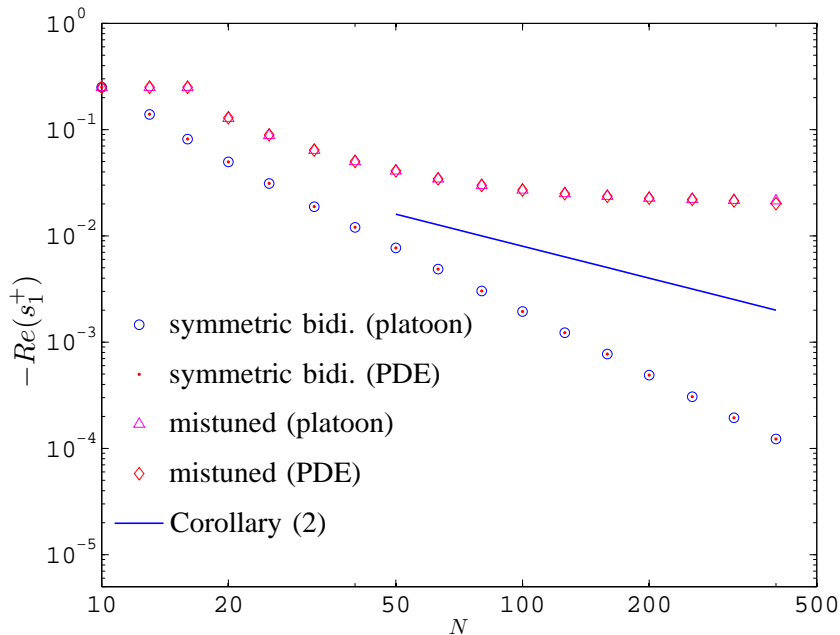


Fig. 6. Stability margin improvement by mistuning in Scenario I. The figure shows the least stable eigenvalue of the closed loop platoon (i.e., of A_{L-F} in (9)) and of the PDE (28) with Dirichlet boundary conditions, with and without mistuning, for a range of values of N . Parameters for the nominal case are $k_0 = 1$ and $b_0 = 0.5$, and the mistuning amplitude is $\epsilon = 0.1$. The mistuned control gains are shown in Figure 5(a). The legend “Corollary 2” refers to the prediction by Corollary 2 for large N .

Theorem 2: Consider the eigenvalue problem for the mistuned PDE (28) with Neumann-Dirichlet boundary condition (18) corresponding to scenario II. The l^{th} eigenvalue pair is given by the asymptotic formula

$$\begin{aligned} s_l^+(\epsilon) &= -\epsilon \frac{l}{4b_0N} \int_0^{2\pi} k_m(x) \sin\left(\frac{lx}{2}\right) dx + O(\epsilon^2) + O\left(\frac{1}{N^2}\right), \\ s_l^-(\epsilon) &= -b_0 + \epsilon \frac{l}{4b_0N} \int_0^{2\pi} k_m(x) \sin\left(\frac{lx}{2}\right) dx + O(\epsilon^2) + O\left(\frac{1}{N^2}\right), \end{aligned}$$

that is valid for each l in the limit as $\epsilon \rightarrow 0$ and $N \rightarrow \infty$. \square

As with scenario I, here again we use the above result to determine the most beneficial profile $k_m(x)$ for small ϵ :

Corollary 3 (Mistuning profile for Scenario II): Consider the problem of minimizing the least-stable eigenvalue of the PDE (28) with Neumann-Dirichlet boundary conditions (18) by choosing $k^{(f,purt)}(x) \in L^\infty([0, 2\pi])$ with norm-constraint $\max_{x \in [0, 2\pi]} |k^{(f,purt)}(x)| = 1$, and $k^{(b,purt)}(x) = -k^{(f,purt)}(x)$. In the limit as $\epsilon \rightarrow 0$, the optimal $k^{(f,purt)}$ is given by $k^{(f,purt)}(x) \equiv 1$. With this profile, the least-stable eigenvalue is given by the asymptotic formula

$$s_1^+(\epsilon) = -\frac{\epsilon}{b_0N}$$

in the limit as $\epsilon \rightarrow 0$ and $N \rightarrow \infty$. \square

The result shows that, as in scenario I, it is possible to improve the closed-loop stability margin in scenario II with an arbitrary small amount of mistuning ϵ such that the least-stable eigenvalue s_1^+ asymptotes to 0 as $O(\frac{1}{N})$ in the mistuned case as opposed to $O(\frac{1}{N^2})$ in the symmetric case. Numerically obtained least stable eigenvalues for the PDE and the platoon state-space model for scenario II are shown in Fig. 7 for a range of values of N . It is clear from the figure that, as in scenario I, the mistuned eigenvalues show an order of magnitude improvement over their values in the symmetric bidirectional case with only $\pm 10\%$ change in the control gains.

Remark 2 (Robustness to small changes from the optimal gains): An advantage of the mistuning design is that mistuned closed loop eigenvalues are robust to small local discrepancies in the control gains from the optimal ones. This can be seen (for scenario I) from the asymptotic eigenvalue formula for s_1^+ in Theorem 1, which shows that one would obtain a $O(\frac{1}{N})$ estimate for any choice of $k_m(x)$ as long as $\int_0^{2\pi} k_m(x) \sin(x) dx \neq 0$. A similar argument holds for scenario II.

C. Simulations

We now present results of a few simulations that show the time-domain improvements – manifested in faster decay of initial errors – with the mistuning-based design of control gains. Simulations were carried out

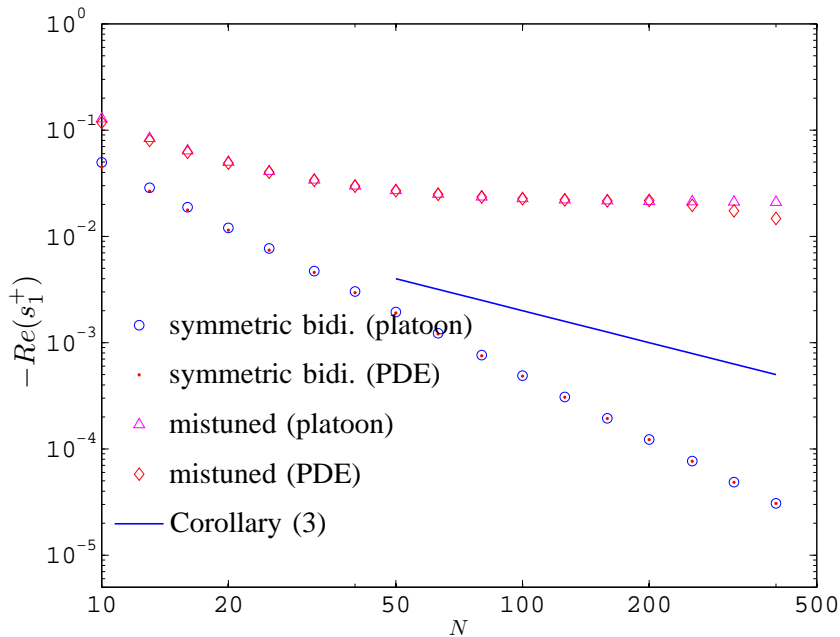


Fig. 7. Stability margin improvement by mistuning in scenario II. The figure shows the least stable eigenvalue of the closed loop platoon (i.e., of A_L in (9)) and of the PDE (28) with Neumann-Dirichlet b.c., with and without mistuning, for a range of values of N . The parameters for the nominal case are $k_0 = 1$ and $b_0 = 0.5$, and the mistuning amplitude is $\epsilon = 0.1$. The mistuned control gains that are used are shown in Figure 5(b). The legend “Corollary 3” refers to the prediction by Corollary 3 of mistuned PDE eigenvalues.

for a platoon of $N = 20$ vehicles with scenario I, i.e., with fictitious lead and follow vehicles. The desired gap was $\Delta = 1$ and desired velocity was $V_d = 5$. The initial velocity of every vehicle was chosen as the desired velocity and the initial position of the i^{th} vehicle was chosen as $Z_i(0) = i\Delta - 0.5$ for $i = \{1, \dots, N\}$. As a result, the initial relative position error and velocity error of every vehicle was zero except for the first vehicle, whose relative position error with respect to the fictitious lead vehicle was 0.5.

Figure 8 depicts the time-histories of the absolute and relative position errors of the individual vehicles with a symmetric bidirectional control, where the control gains were chosen as $k_i^{(f)} = k_i^{(b)} = 1$ and $b_i = 0.5$ for $i = \{1, \dots, 20\}$. The absolute position error of the i^{th} vehicle is $Z_i - Z_i^d$ and the relative position error is $Z_{i-1} - Z_i - \Delta$.

Figure 9 depicts the time-histories of the absolute and relative position errors for the platoon with mistuned controller gains. The mistuning gains used for the simulation are the ones shown in Figure 5(a) (chosen according to Corollary 2) so that maximum and minimum gains over all vehicles are within $\pm 10\%$ of the nominal value. On comparing Figures 8 and 9, we see that the errors in the initial conditions are reduced faster

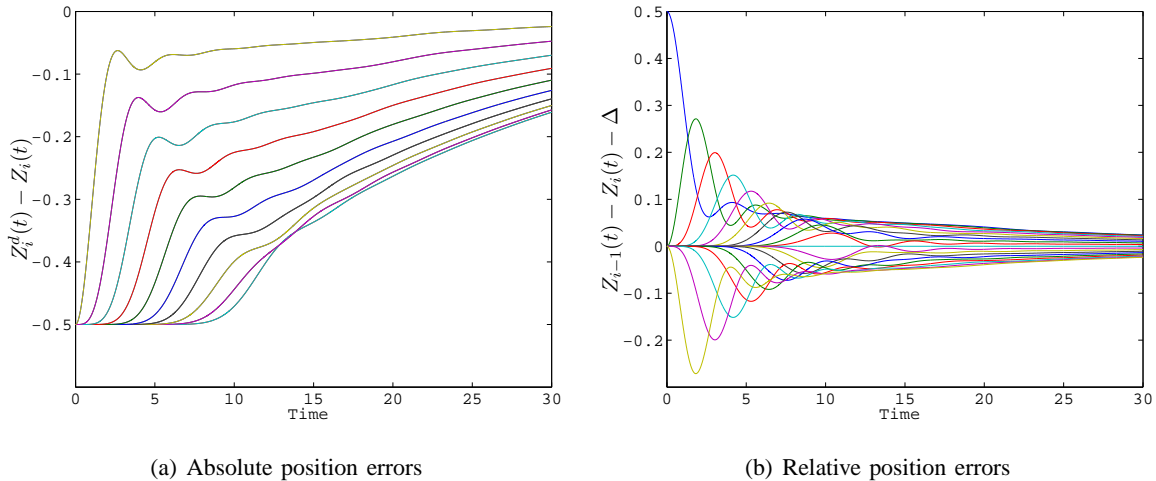


Fig. 8. Performance of symmetric bidirectional control: time histories of the absolute and relative position errors of the vehicles in a platoon with symmetric bidirectional control (scenario I). The control gains are $k_i^{(f)} = k_i^{(b)} = 1$ and $b_i = 0.5$ for every $i = 1, \dots, 20$.

in the mistuned case compared to the nominal case. These observations are consistent with the improvement in the closed-loop stability margin with the mistuned design.

VI. DISCUSSION ON MISTUNING DESIGN

There are several remarks to be made regarding the mistuning based design. We first comment on the implementation issues, in particular, on the effect of small platoon size on the proposed design, and on the information requirements for its implementation.

A. Large vs. small N

The PDE model is developed for large N . However, detailed numerical comparisons presented above (see Figures 3, 6 and 7) show that the PDE model provides quantitatively correct predictions about the discrete platoon dynamics even for small values of N . The PDE has an infinite number of eigenvalues as opposed to a finite number for the discrete platoon. So, one can not expect an exact match. However, PDE eigenvalues exactly match the least stable and other dominant eigenvalues of the discrete platoon (see Figure 2 and Figure 10). In a similar vein, the benefits of mistuning are also realized for relatively small values of N . For example, when the number of vehicles is 20, a mistuning of $\pm 10\%$ results in an improvement of 150% (from -0.0491 to -0.1281) in scenario I and an improvement of 400% (from -0.012 to -0.05) in scenario II over the symmetric case.

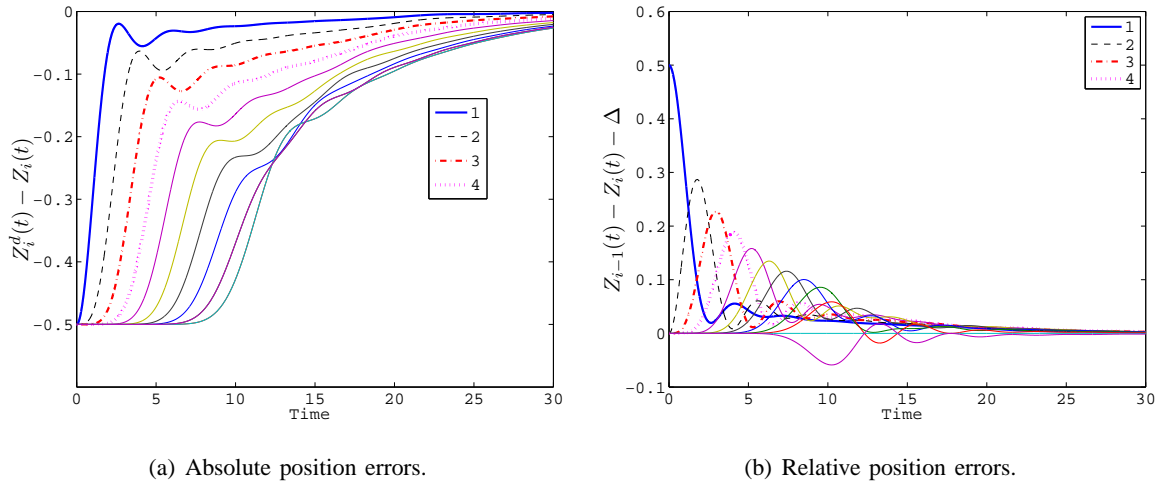


Fig. 9. Performance of mistuned control: time histories of the absolute and relative position errors of the vehicles in a platoon (scenario I) with mistuned bidirectional control. The control gains used are those shown in Figure 5(a). The legends refer to the vehicle indices.

B. Information requirements

In order to implement the mistuned controller gains designed above, every vehicle needs the following information (in addition to what is needed to use a symmetric bidirectional control): (1) the mistuning amplitude ϵ , and (2) in scenario I, whether it is in the front half of the platoon or not. This information can be provided to the vehicles in advance. Note that in scenario II, only the value of ϵ is needed.

It is possible that due to vehicles leaving and joining the platoon, information on whether a vehicle belongs to the front half of the platoon may become erroneous with time, especially for the vehicles that are close to the middle. In scenario I, such error may lead to a non-optimal gains used by the vehicles. However, since the improvement in closed loop stability margin due to mistuning is robust to small deviations in the gains from the optimal ones (see Remark 2), errors in determining whether a vehicle belongs to the front half of the platoon or not will not greatly affect the improvement in stability margin. Note that in scenario II this issue does not even arise.

C. Large asymmetry

Although the mistuning profiles described in Corollaries 2 and 3 are optimal in the limit as $\epsilon \rightarrow 0$, one would like to be able to use them with somewhat larger values of ϵ to realize the benefit of mistuning. To do so, one has to preclude the possibility of “eigenvalue cross-over”, i.e., of the second (s_2^+) or some other marginally stable eigenvalue from becoming the least stable eigenvalue in the presence of mistuning. It turns out that such a cross-over is ruled out as a consequence of the Sturm-Liouville (S-L) theory for the elliptic

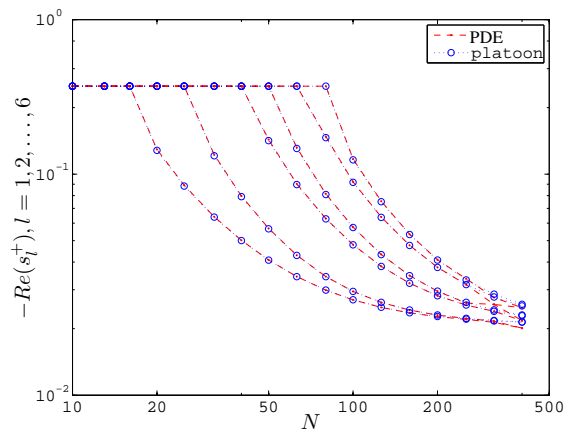


Fig. 10. The real parts of six eigenvalues (closest to 0) of the closed loop platoon dynamics for Scenario I, and their comparison with the PDE eigenvalues with Dirichlet-Dirichlet boundary conditions, with controller gains mistuned as those shown in Figure 5. As predicted by Sturm-Liouville theory, the least stable eigenvalue stays the least stable, although eigenvalues that are more stable merge with it as N increases.

boundary value problems. The standard argument relies on the positivity of the eigenfunction corresponding to s_1^+ ; the reader is referred to [31] for the details. Figure 10 verifies this numerically by depicting the six eigenvalues closest to 0 (for both the PDE and the discrete platoon) as a function of N when mistuning is applied.

D. Sensitivity to disturbance

Automated platoons suffer from high sensitivity to external disturbances; which is referred to as “string instability” or “slinky-type effects” [1, 14, 19]. Here we provide numerical evidence that mistuning also helps in reducing the sensitivity to disturbances.

When external disturbances are present, we model the dynamics of vehicle i by $\ddot{Z}_i = U_i + W_i$, where W_i is the external disturbance acting on the vehicle. In the y coordinates, the vehicle dynamics become $\ddot{y}_i = u_i + w_i$, where $w_i := 2\pi W_i/L$. In scenario I, the state space model of the entire platoon becomes,

$$\dot{\psi} = A_{L-F} \psi + \underbrace{\begin{bmatrix} \mathbf{0} \\ I \end{bmatrix}}_{\mathcal{B}} \mathbf{w}, \quad (29)$$

$$\mathbf{e} = C\psi$$

where $\psi = [\tilde{\mathbf{y}}^T, \tilde{\mathbf{v}}^T]^T$, A_{L-F} , $\mathbf{w} = [w_1, w_2, \dots, w_N]^T$, and $\mathbf{e} := [e_1^{(f)}, \dots, e_N^{(f)}]^T$ is a vector of front spacing errors $e_i^{(f)} := \tilde{y}_{i-1} - y_i$.

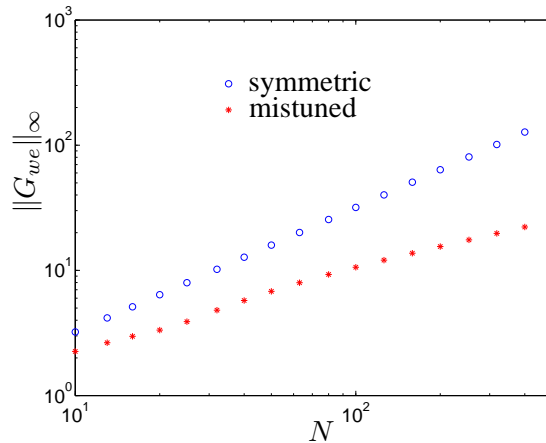


Fig. 11. H_∞ norm of the transfer function G_{we} from disturbance \mathbf{w} to spacing error \mathbf{e} in (29), with and without mistuning, for scenario I. The mistuned gains used are shown in Figure 5(a). Norms are computed using the Control Systems Toolbox in MATLAB[©].

The H_∞ norm of the transfer function G_{we} from the disturbance \mathbf{w} to the inter-vehicle spacing errors \mathbf{e} is a measure of the closed loop's sensitivity to external disturbances [7, 12]. Figure 11 shows a plot of the H_∞ norm of G_{we} as a function of N , with and without mistuning. The mistuning profile used is the same as the one used for the eigenvalue trends reported in Figure 6. It is clear from the figure that $\pm 10\%$ mistuning results in large reduction of the H_∞ norm of G_{we} . Although this reduction is more pronounced for large N , it is still significant for small N . In particular, for $N = 20$, a 10% mistuning yields approximately 50% reduction in the H_∞ norm (from 6.69 to 3.38). Detailed analysis of the effect of mistuning on sensitivity to disturbances will be a subject of future work.

VII. CONCLUSION

We developed a PDE model that describes the closed loop dynamics of an N -vehicle platoon with a decentralized bidirectional control architecture. Analysis of the PDE model revealed several important features of the problem. First, we showed that when every vehicle uses the same controller with constant gain that is independent of N (the so-called symmetric bidirectional architecture), the least stable eigenvalue of the closed loop decays to 0 as $O(\frac{1}{N^2})$. Second, and more significantly, analysis of the PDE suggested a way to ameliorate this progressive loss of stability margin, by introducing small amounts of “mistuning”, i.e., by changing the controller gains from their nominal symmetric values. We proved that with arbitrary small amounts of mistuning, the decay of the least stable closed loop eigenvalue can be improved to $O(\frac{1}{N})$. Several

comparisons with the numerically computed eigenvalues of state-space model of the platoon corroborate the predictions of the PDE-based analysis.

Although the PDE model is derived under the assumption that the number of vehicles, N , is large, in practice the PDE provides quantitatively correct predictions for the discrete platoon dynamics even for relatively small values of N . The amount of information that is needed to implement the mistuned control gains (over that in the symmetric bidirectional architecture) is quite small and need to be provided only once. Furthermore, the stability improvement due to mistuning is robust to small errors (between the actual gains used and the optimal mistuned gains) that may occur in practice due to changes in the number of vehicles in the platoon over time.

The advantage of the PDE formulation is reflected in the ease with which the closed loop eigenvalues are obtained for two different boundary conditions, with lead and follow vehicles as well as with only a lead vehicle. Certain important aspects of the problem, such as the beneficial nature of forward-backward asymmetry in control gains, is revealed by the PDE while they are difficult to see with the (spatially) discrete, state-space model.

Numerical calculations show that the mistuning design also reduces sensitivity to disturbances of the closed-loop platoon. Analysis of the beneficial effect of mistuning in reducing sensitivity to external disturbances is a subject of future research. In the future, we also plan to examine PDE-based models for modeling and analysis of fleet of vehicles as in 2 or 3 spatial dimensions.

REFERENCES

- [1] S. Darbha, J. K. Hedrick, C. C. Chien and P. Ioannou. A comparison of spacing and headway control laws for automatically controlled vehicles. *Vehicle System Dynamics*, vol. 23: 597–625, 1994.
- [2] J. K. Hedrick, M. Tomizuka and P. Varaiya. Control issues in automated highway systems. *IEEE Control Systems Magazine*, vol. 14: 21 – 32, 1994.
- [3] R. E. Chandler, R. Herman and E. W. Montroll. Traffic dynamics: Studies in car following. *Operations Research*, vol. 6, no. 2: 165–184, 1958.
- [4] W. S. Levine and M. Athans. On the optimal error regulation of a string of moving vehicles. *IEEE Transactions on Automatic Control*, vol. AC-11, no. 3: 355–361, 1966.
- [5] S. M. Melzer and B. C. Kuo. A closed-form solution for the optimal error regulation of a string of moving vehicles. *IEEE Transactions on Automatic Control*, vol. AC-16, no. 1: 50–52, 1971.
- [6] M. R. Jovanović and B. Bamieh. On the ill-posedness of certain vehicular platoon control problems. *IEEE Transactions on Automatic Control*, vol. 50, no. 9: 1307 – 1321, 2005.

- [7] P. Seiler, A. Pant and J. K. Hedrick. Disturbance propagation in vehicle strings. *IEEE Transactions on Automatic Control*, vol. 49: 1835–1841, 2004.
- [8] J. D. Wolfe, D. F. Chichkat and J. L. Speyer. Decentralized controllers for unmaned aerial vehicle formation flight. In *Guidance, Navigation and Control Conference*, pp. July 29–31. 1996.
- [9] P. K. C. Wang, F. Y. Hadaegh and K. Lau. Synchronized formation rotation and attitude control of multiple free-flying spacecraft. *Journal of Guidance, Control, and Dynamics*, vol. 22, no. 1: 28–35, 1999.
- [10] S. S. Stankovic, M. J. Stanojevic and D. D. Siljak. Decentralized overlapping control of a platoon of vehicles. *IEEE Transactions on Control Systems Technology*, vol. 8: 816–832, 2000.
- [11] L. E. Peppard. String stability of relative-motion PID vehicle control systems. *IEEE Transactions on Automatic Control*, pp. 579–581, 1974.
- [12] P. Barooah and J. P. Hespanha. Error amplification and distrubance propagation in vehicle strings. In *Proceedings of the 44th IEEE conference on Decision and Control*. 2005.
- [13] K. C. Chu. Decentralized control of high-speed vehicle strings. *Transportation Science*, vol. 8: 361–383, 1974.
- [14] Y. Zhang, E. B. Kosmatopoulos, P. A. Ioannou and C. C. Chien. Autonomous intelligent cruise control using front and back information for tight vehicle following maneuvers. *IEEE Transactions on Vehicular Technology*, vol. 48: 319–328, 1999.
- [15] S. E. Shladover. Longitudinal control of automotive vehicles in close-formation platoons. *Journal of Dynamic systems, Measurements and Control*, vol. 113: 302–310, 1978.
- [16] H.-S. Tan, R. Rajamani and W.-B. Zhang. Demonstration of an automated highway platoon system. In *American Control Conference*, vol. 3, pp. 1823 – 1827. 1998.
- [17] X. Liu, S. S. Mahal, A. Goldsmith and J. K. Hedrick. Effects of communication delay on string stability in vehicle platoons. In *IEEE International Conference on Intelligent Transportation Systems (ITSC)*. 2001.
- [18] P. Barooah, P. G. Mehta and J. P. Hespanha. Control of large vehicular platoons: Improving closed loop stability by mistuning. In *The 2007 American Control Conference*, pp. 4666–4671. July.
- [19] S. Darbha and J. K. Hedrick. String stability of interconnected systems. *IEEE Transactions on Automatic Control*, vol. 41, no. 3: 349–356, 1996.
- [20] S. K. Yadlapalli, S. Darbha and K. R. Rajagopal. Information flow and its relation to stability of the motion of vehicles in a rigid formation. *IEEE Transactions on Automatic Control*, vol. 51, no. 8, 2006.
- [21] B. Shapiro. A symmetry approach to extension of flutter boundaries via mistuning. *Journal of Propulsion and Power*, vol. 14, no. 3: 354–366, 1998.

- [22] O. O. Bendiksen. Localization phenomena in structural dynamics. *Chaos, Solitons, and Fractals*, vol. 11: 1621–1660, 2000.
- [23] A. J. Rivas-Guerra and M. P. Mignolet. Local/global effects of mistuning on the forced response of bladed disks. *Journal of Engineering for Gas Turbines and Power*, vol. 125: 1–11, 2003.
- [24] P. G. Mehta, G. Hagen and A. Banaszuk. Symmetry and symmetry breaking for a wave equation with feedback. *SIAM Journal of Dynamical Systems*, vol. 6, no. 3: 549–575, 2007.
- [25] M. Lighthill and G. Whitham. On kinematic waves II: a theory of traffic flow on long crowded roads. In *Royal Society, London Series A*. 1955.
- [26] D. Helbing. Traffic and related self-driven many-particle systems. *Review of Modern Physics*, vol. 73: 1067–1141, 2001.
- [27] D. Jacquet, C. C. de Wit and D. Koenig. Traffic control and monitoring with a macroscopic model in the presence of strong congestion waves. In *44th IEEE Conference on Decision and Control & European Control Conference*, pp. 2164–2169. 2005.
- [28] P. Y. Li, R. Horowitz, L. Alvarez, J. Frankel, *et al.*. An automated highway system link layer controller for traffic flow stabilization. *Transportation Research, Part C*, vol. 5, no. 1: 11–37, 1997.
- [29] L. Alvarez, R. Horowitz and P. Li. Traffic flow control in automated highway systems. *Control Engineering Practice*, vol. 7: 1071–1078, 1999.
- [30] C. Canuto, M. Y. Hussaini, A. Quarteroni and T. A. Zang. *Spectral Methods in Fluid Dynamics*. Springer Series in Computational Physics. Springer-Verlag, New York, 1983.
- [31] L. C. Evans. *Partial Differential Equations*, vol. 19 of *Graduate Studies in Mathematics*. American Mathematical Society, 1998.
- [32] A. Pazy. *Semigroups of linear operators and applications to partial differential equations*, vol. 44 of *Applied Mathematical Sciences*. Springer-Verlag, New York, 1983. ISBN 0-387-90845-5.

APPENDIX I

TECHNICAL RESULTS

A. Solution properties of PDE (15).

In this section, we use the semigroup theory to obtain results on well-posedness of the PDE (15). To apply these methods, we first re-write the PDE as a first order evolution equation:

$$\begin{aligned} \frac{\partial \tilde{\rho}}{\partial t} &= -\rho_0 \frac{\partial \tilde{v}}{\partial x} \\ \frac{\partial \tilde{v}}{\partial t} &= -\left[\frac{1}{\rho_0^2} k_1(x) \tilde{\rho} + \frac{1}{2\rho_0^3} \frac{\partial}{\partial x} (\tilde{\rho} k_0(x)) + b \tilde{v} \right] := A \begin{bmatrix} \tilde{\rho} \\ \tilde{v} \end{bmatrix}, \end{aligned} \quad (30)$$

where A is a linear operator; $k_0(x) := k^+(x)$ and $k_1(x) := k^-(x) - \frac{1}{2\rho_0} \frac{dk^+}{dx}(x)$. We will assume these coefficients $k_0(x), k_1(x) \in L^\infty([0, 2\pi])$ and $k_0(x) > 0$. $\tilde{\rho}$ has the units of and the physical interpretation of

density perturbation.

Using (30), we denote the initial/boundary value problem as:

$$\begin{aligned} \dot{z}(x, t) &= Az(x, t) \quad \text{for } x \in X, \quad t > 0 \\ z(x, 0) &= z_0(x), \end{aligned} \tag{31}$$

where $z(x, t) := [\tilde{\rho}(x, t), \tilde{v}(x, t)]$, $z_0(x) = [\tilde{\rho}_0(x), \tilde{v}_0(x)]$ and A is defined in (30); $\tilde{\rho}_0$ and \tilde{v}_0 will be assumed to functions in appropriately defined Banach spaces. The main goal of this section will be to show that the solution for the linear problem (30) can be expressed in terms of a C^0 semigroup provided eigenvalues of the operator A satisfy appropriate bounds. We begin with a discussion of the notation.

Preliminaries and Notation. We denote $z := [\tilde{\rho}, \tilde{v}]$, $L^2(X)$ denotes the Hilbert space of square integrable functions on X ($\|\tilde{v}\|_{L^2}^2 := \int \tilde{v}^2 dx$), H^k denotes the Sobolev space of functions such that derivatives up to k^{th} -order exist in a weak sense and belong to $L^2(X)$ (the Sobolev norm is denoted by $\|\cdot\|_{H^k}$), and H_0^1 denotes the Sobolev space H^1 of functions that satisfy the Dirichlet boundary condition. We denote $Z := L^2 \times L^2$, and equip it with a norm $\|\cdot\|$. Let $\mathcal{D}(A) := H^1 \times (H_0^1 \cap L^2)$ and consider the right hand side of evolution equation (30) as an unbounded but closed densely defined linear operator

$$A : \mathcal{D}(A) \subset Z \rightarrow Z. \tag{32}$$

A real number s belongs to $\rho(A)$, the resolvent set for A , provided the operator $sI - A : \mathcal{D}(A) \rightarrow Z$ is 1-1 and onto. For $s \in \rho(A)$, the resolvent operator $R_s := (sI - A)^{-1}$. Finally, we recall that a one-parameter family of linear operators $\{S(t)\}_{t \geq 0}$ is a C^0 -semigroup if 1) $S(0)z = z$ for all $z \in Z$, 2) $S(t+s)z = S(t)S(s)z$ for all $t, s \geq 0$ and $z \in Z$, and 3) the mapping $t \rightarrow S(t)z$ is continuous from $[0, \infty)$ into Z . A C^0 semigroup is a contraction semigroup if $\|S(t)z\| \leq \|z\|$ for all $t \geq 0$. The Hille-Yosida theorem states that a closed densely defined linear operator A is the generator of a contraction semigroup if and only if

$$(0, \infty) \subset \rho(A) \quad \text{and} \quad \|R_s z\| \leq \frac{1}{s} \|z\| \quad \forall z \in Z. \tag{33}$$

Our strategy will be to apply Hille-Yosida theorem to deduce solution properties of the evolution equation (31). Following closely the development in [31], there are three steps to accomplish this: 1) we show that A is a densely defined closed linear operator on Z , 2) characterize the resolvent set by considering the eigenvalue problem, and 3) show the bound (33) for the resolvent. Step 2 will lead to an eigenvalue problem, whose analysis and optimization is the subject of this paper. We present details for the three steps next:

- 1) The domain of A , $\mathcal{D}(A)$, is dense in Z because H^1 is dense in L^2 . To show A is closed, consider a

sequence $\{\tilde{\rho}_m, \tilde{v}_m\} \subset \mathcal{D}(A)$ such that

$$(\tilde{\rho}_m, \tilde{v}_m) \xrightarrow{Z} (\tilde{\rho}, \tilde{v}) \quad (34)$$

$$A(\tilde{\rho}_m, \tilde{v}_m) \xrightarrow{Z} (f, g), \quad (35)$$

where the arrow notation denotes the fact that the convergence is in $Z = L^2 \times L^2$. Since $\tilde{v}_m \xrightarrow{L^2} \tilde{v}$ so $-\rho_0 \frac{\partial \tilde{v}}{\partial x} = f \in L^2$, i.e., $\tilde{v} \in H^1$. Now, $\{\tilde{v}_m\}$ is Cauchy in L^2 by (34) and $\{\frac{\partial \tilde{v}_m}{\partial x}\}$ is Cauchy in L^2 by (35) and

$$\|\tilde{v}_m - \tilde{v}_l\|_{H^1} \leq C \left(\left\| \frac{\partial \tilde{v}_m}{\partial x} - \frac{\partial \tilde{v}_l}{\partial x} \right\|_{L^2} + \|\tilde{v}_m - \tilde{v}_l\|_{L^2} \right), \quad (36)$$

so $\{\tilde{v}_m\}$ is Cauchy in H^1 and $\tilde{v}_m \xrightarrow{H^1} \tilde{v}$. By repeating essentially the same argument, one also finds that $\tilde{\rho} \in H^1$ and $\tilde{\rho}_m \xrightarrow{H^1} \tilde{\rho}$. Consequently, $A(\tilde{\rho}_m, \tilde{v}_m) \xrightarrow{Z} A(\tilde{\rho}, \tilde{v})$ and $A(\tilde{\rho}, \tilde{v}) = (f, g)$.

2) Let $s > 0$, $(f, g) \in Z = L^2 \times L^2$, and consider the operator equation

$$(sI - A) \begin{bmatrix} \tilde{\rho} \\ \tilde{v} \end{bmatrix} = \begin{bmatrix} f \\ g \end{bmatrix}. \quad (37)$$

This is equivalent to two scalar equations

$$s\tilde{\rho} + \rho_0 \frac{\partial \tilde{v}}{\partial x} = f \quad (\tilde{\rho} \in L^2 \cap H^1), \quad (38)$$

$$s\tilde{v} + \left[\frac{1}{\rho_0^2} k_1(x) \tilde{\rho} + \frac{1}{2\rho_0^3} \frac{\partial}{\partial x} (k_0(x) \tilde{\rho}) + b\tilde{v} \right] = g \quad (\tilde{v} \in L^2 \cap H_0^1). \quad (39)$$

Using the first equation to write $s\tilde{\rho} = -\rho_0 \frac{\partial \tilde{v}}{\partial x} + f$, this implies

$$s^2 \tilde{v} + bs\tilde{v} + L\tilde{v} = h, \quad (40)$$

where

$$L\tilde{v} := \frac{1}{2\rho_0^2} \frac{\partial}{\partial x} (-k_0(x) \frac{\partial \tilde{v}}{\partial x}) - \frac{1}{\rho_0} (k_1(x) \frac{\partial \tilde{v}}{\partial x}) \quad (41)$$

is an elliptic operator (because $k_0(x) > 0$ for all $x \in X$) and $h = sg - \frac{1}{2\rho_0^3} \frac{\partial}{\partial x} (k_0(x)f) - \frac{1}{\rho_0^2} k_1(x)f$ (note that $h \in H^{-1}(X)$). Consequently, solutions of ((37)) can be studied in terms of solutions of ((41)). The spectrum of A is completely characterized by the spectrum of L . We will obtain spectral bounds, dependent upon $k_0(x)$ and $k_1(x)$, in the following sections. In particular, we will establish that $\text{Real}[s] < \alpha$ for some $\alpha < 0$ and thus $\rho(A) \supset (\alpha, \infty)$. For $k_1(x) = 0$, it turns out that $[0, \infty) \subset \rho(A)$ for any choice of positive $k_0(x)$ (this is also clear from the symmetric eigenvalue problem (41)).

3) If a positive $s \in \rho(A)$, there exists a unique solution $(\tilde{\rho}, \tilde{v}) \in Z$ for (38)-(39) via the theory of elliptic operators: solve (40) to obtain $\tilde{v} \in H_0^1$ and $s\tilde{\rho} = -\rho_0 \frac{\partial \tilde{v}}{\partial x} + f$. We write the solution as $(\tilde{\rho}, \tilde{v}) = R_s(f, g)$, define a bilinear form

$$B[\tilde{\rho}, s] := \frac{1}{2\rho_0^4} \int_X k_0(x) \tilde{\rho}(x) s(x) dx, \quad (42)$$

for $\tilde{\rho}, s \in L^2$ and consider an equivalent norm (on Z) for solutions $(\tilde{\rho}, \tilde{v})$ as:

$$\|(\tilde{\rho}, \tilde{v})\| := B[\tilde{\rho}, \tilde{\rho}] + \|\tilde{v}\|_{L^2} \quad (43)$$

To obtain the resolvent bound, we multiply (39) by \tilde{v} and use integration by parts:

$$s(\|\tilde{v}\|_{L^2} + B[\tilde{\rho}, \tilde{\rho}]) + b\|\tilde{v}\|_{L^2} + \frac{1}{\rho^2} \int k_1(x) \tilde{\rho} \tilde{v} dx = \int g \tilde{v} dx + B[\tilde{\rho}, f]. \quad (44)$$

In general, the bound depends upon $k_1(x)$. For $k_1(x) = 0$, we have

$$s\|(\tilde{\rho}, \tilde{v})\|^2 \leq (s + b)\|\tilde{v}\|_{L^2} + B[\tilde{\rho}, \tilde{\rho}] = \int g \tilde{v} dx + B[\tilde{\rho}, f] \leq \|(f, g)\| \cdot \|(\tilde{\rho}, \tilde{v})\|, \quad (45)$$

where the first inequality holds because $s > 0$ and $b > 0$ and the last inequality follows from the generalized Cauchy-Schwarz inequality. As a result, $\|R_s(f, g)\| \leq \frac{1}{s}\|(f, g)\|$ and $\|R_s\| \leq \frac{1}{s}$.

For the general case where $k_1(x)$ is not identically zero, one expresses the operator

$$A = A_0 + \tilde{A}, \quad (46)$$

where

$$A_0 \begin{bmatrix} \tilde{\rho} \\ \tilde{v} \end{bmatrix} = \begin{bmatrix} 0 & -\rho_0 \frac{\partial}{\partial x} \\ -\frac{1}{2\rho_0^3} \frac{\partial}{\partial x} (k_0(x) \cdot) & -b \end{bmatrix} \begin{bmatrix} \tilde{\rho} \\ \tilde{v} \end{bmatrix}, \quad \tilde{A} \begin{bmatrix} \tilde{\rho} \\ \tilde{v} \end{bmatrix} = \begin{bmatrix} 0 & 0 \\ -\frac{1}{\rho_0^2} k_1(x) & 0 \end{bmatrix} \begin{bmatrix} \tilde{\rho} \\ \tilde{v} \end{bmatrix}. \quad (47)$$

In words, A_0 is the operator with $k_1(x) = 0$ and \tilde{A} is the operator due to $k_1(x)$. We note that \tilde{A} is a bounded perturbation of A_0 (on Z). We have already showed the existence of a C^0 -semigroup for A_0 . For the general operator A , the existence follows from using a perturbation theorem (see Theorem 1.1 in Ch. 3 of [32]).

B. Proof of Theorem 1

Proof of Theorem 1. The spatial inhomogeneity introduced by the x -dependent coefficients $k_m(x)$ and $k_s(x)$ destroy the spatial invariance of the nominal PDE (20). Hence, the Fourier basis – eigenfunctions of the Laplacian – no longer lead to a diagonalization of the mistuned PDE. The methods of section IV thus need to be suitably modified. In order to compute the eigenvalues for the mistuned PDE (28), we take a Laplace transform of (28) and get

$$-a_0^2 \frac{\partial^2 \eta}{\partial x^2} + s^2 \eta + b_0 s \eta = \epsilon \left[\frac{k_m}{\rho_0} \frac{\partial \eta}{\partial x} + \frac{k_s}{2\rho_0^2} \frac{\partial^2 \eta}{\partial x^2} \right], \quad (48)$$

where $\eta(x)$ is the Laplace transform (with respect to t) of $\tilde{v}(x, t)$. We are interested in eigenvalues of (48) with Dirichlet boundary conditions, i.e., the values of s for which a solution to the homogeneous PDE (48)

exists with boundary conditions $\eta(0) = \eta(2\pi) = 0$. To obtain these eigenvalues, we use a perturbation method expressing the eigenfunction and eigenvalue in a series form:

$$\eta(x) = \eta_0(x) + \epsilon\eta_1(x) + O(\epsilon^2), \quad (49)$$

$$s = r_0 + \epsilon r_1 + O(\epsilon^2). \quad (50)$$

We note that ϵr_1 denotes the perturbation to the nominal eigenvalue r_0 as a result of the mistuning. Substituting (50) in (48) and doing an $O(1)$ balance, we get

$$O(1) : \quad -a_0^2(\eta_0)_{xx} + r_0^2\eta_0 + br_0\eta_0 = 0, \quad (51)$$

whose eigen-solution is given by

$$\eta_0 = d_l \sin\left(\frac{lx}{2}\right), \quad (52)$$

$$r_0 = s_l^\pm(0), \quad (53)$$

where $l = 1, 2, \dots$, d_l is an arbitrary real constant, and $s_l^\pm(0)$ is given by (24). Next,

$$O(\epsilon) : \quad \left(-a_0^2 \frac{\partial^2}{\partial x^2} + (r_0^2 + b_0 r_0)\right) \eta_1 = + \frac{k_m}{\rho_0} \frac{\partial \eta_0}{\partial x} + \frac{k_s}{2\rho_0^2} \frac{\partial^2}{\partial x^2} \eta_0 - (2r_0 r_1 + b_0 r_1) \eta_0 \\ := R \quad (54)$$

Substituting $r_0 = s_l^\pm(0)$ on the left hand side leads to a resonance condition for the right hand side term, denoted by R . In particular for a solution η_1 to exist, R must lie in the range space of the linear operator

$$\left(-a_0^2 \frac{\partial^2}{\partial x^2} + (r_0^2 + br_0)\right). \quad (55)$$

For this self-adjoint operator, the range space is the complement of its null space $\{\sin(\frac{lx}{2})\}$. This gives the resonance condition as

$$\langle R, \sin\left(\frac{lx}{2}\right) \rangle = 0,$$

where $\langle \cdot, \cdot \rangle$ denotes the standard inner product in $L^2(0, 2\pi)$. Explicitly, this leads to an equation

$$(2r_0 + b_0)r_1 = \frac{l}{4\pi\rho_0} \int_0^{2\pi} k_m(x) \sin(lx) dx - \frac{l^2}{8\pi\rho_0^2} \int_0^{2\pi} k_s(x) \sin^2\left(\frac{lx}{2}\right) dx \quad (56)$$

For values of $r_0 = s_l^\pm(0)$, where $s_l^\pm(0)$ is given by (24), the equation above leads to an expression for perturbation in the two eigenvalues. We denote these perturbations as r_1^\pm . For $r_0 = s_l^+(0)$, we have from Lemma 1 that $b_0 \gg |2r_0|$ when $l \ll l_c$, which happens for every l as $N \rightarrow \infty$ (see eq. (25)), so that

$$r_1^+ \approx \frac{l}{4\pi\rho_0 b_0} \int_0^{2\pi} k_m(x) \sin(lx) dx + O\left(\frac{1}{N^2}\right). \quad (57)$$

Note that we have dropped the second integral on the right hand side of (56) because $\frac{1}{\rho_0^2} = O(1/N^2)$ for large N . For $r_0 = s_k^-(0)$, $2r_0 \approx -2b_0$ for $l \ll l_c$ and

$$r_1^- \approx -\frac{l}{4\pi\rho_0 b_0} \int_0^{2\pi} k_m(x) \sin(lx) dx + O\left(\frac{1}{N^2}\right). \quad (58)$$

Note that

$$r_1^+ + r_1^- = 0.$$

Putting the formulas for the perturbation to the eigenvalues (57) and (58) in (50), we get

$$\begin{aligned} s_l^+(\epsilon) &\approx s_l^+(0) + \epsilon \frac{l}{4\pi b_0 \rho_0} \int_0^{2\pi} k_m(x) \sin(lx) dx + O(\epsilon^2) + O\left(\frac{1}{N^2}\right), \\ s_l^-(\epsilon) &\approx -b_0 - \epsilon \frac{l}{4\pi b_0 \rho_0} \int_0^{2\pi} k_m(x) \sin(lx) dx + O(\epsilon^2) + O\left(\frac{1}{N^2}\right). \end{aligned}$$

Since $s_l^+(0) = O\left(\frac{1}{N^2}\right)$ for $l < l_c$ (Lemma 1) and $\rho_0 = \frac{N}{2\pi}$, the result follows. ■